Model-independent fits to experimental and lattice data for $B \to D^* \ell \bar{\nu}$ (and other) exclusive decays

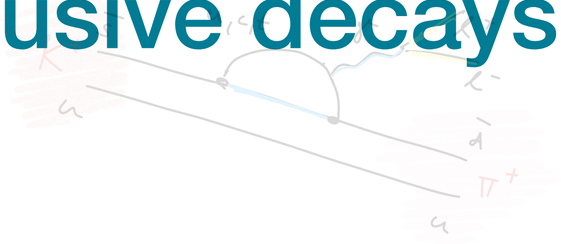

Challenges in Semileptonic Decays
Campus Akademie, Wien

23.09.2024

Andreas Jüttner

CERN
University of Southampton

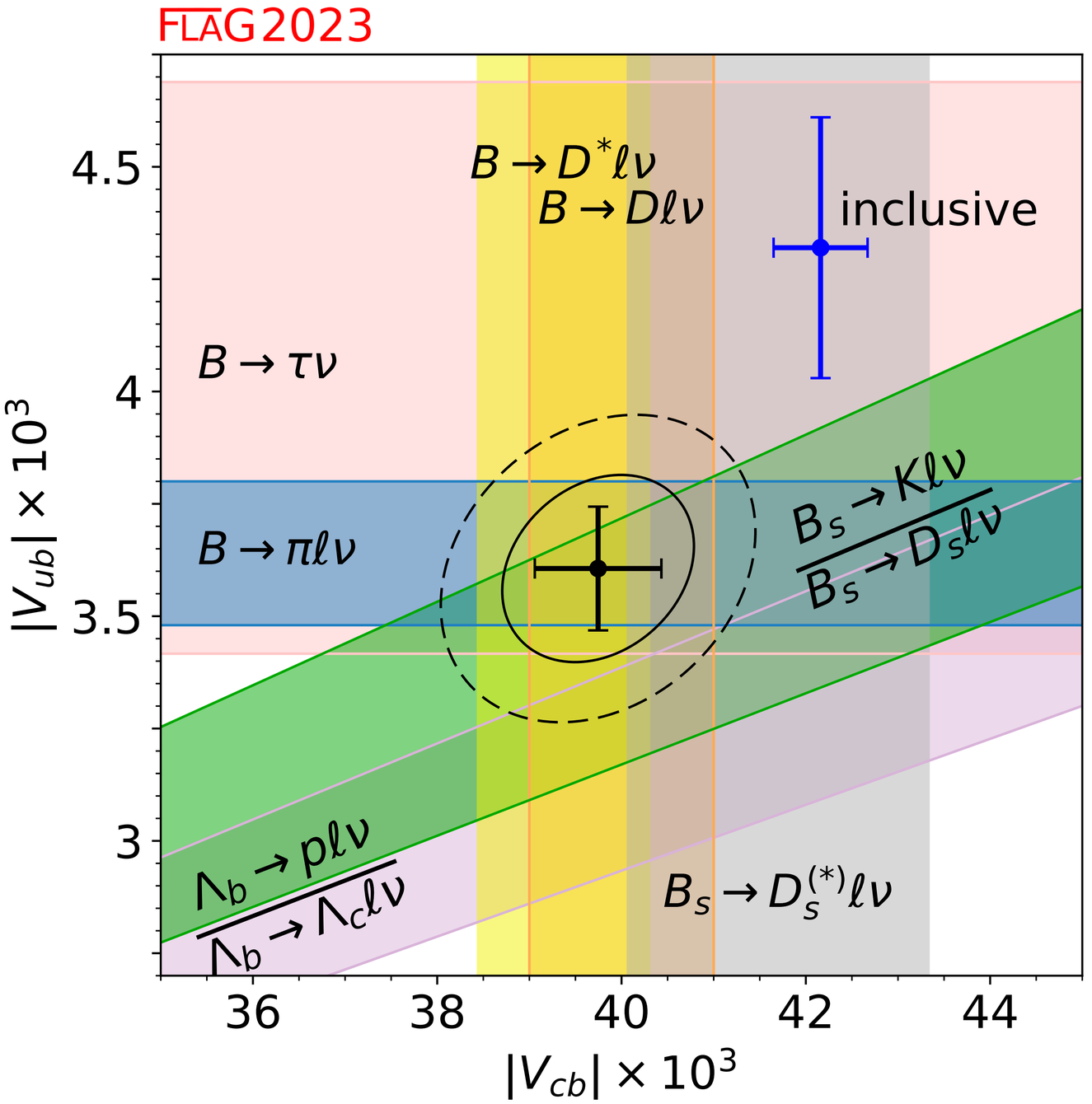
FLAG2023
$B \to D^* \ell\nu$
$B \to D \ell\nu$
inclusive
$B \to \tau\nu$
$B \to \pi \ell\nu$
$\frac{B_s \to K\ell\nu}{B_s \to D_s \ell\nu}$
$\frac{\Lambda_b \to p\ell\nu}{\Lambda_b \to \Lambda_c \ell\nu}$
$B_s \to D_s^{(*)} \ell\nu$
$|V_{ub}| \times 10^3$
$|V_{cb}| \times 10^3$
4.5
4
3.5
3
36
38
40
42
44

Intro: exclusive semileptonic meson decay

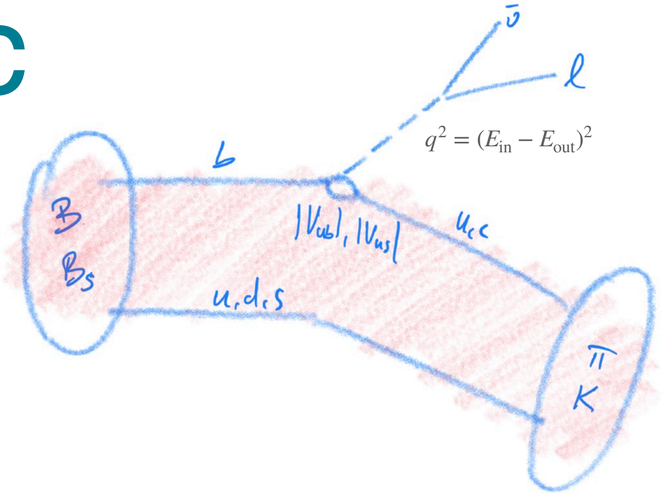

Objective: obtain model-independent theory prediction over entire kinematical range

Input:

- sum rules: $q^2 \approx 0$
- lattice QCD:
  - finite lattice spacing (UV)
  - finite volume (IR)
  - worsening signal-to-noise

→ limited kinematic reach

↓ need extra/interpolation

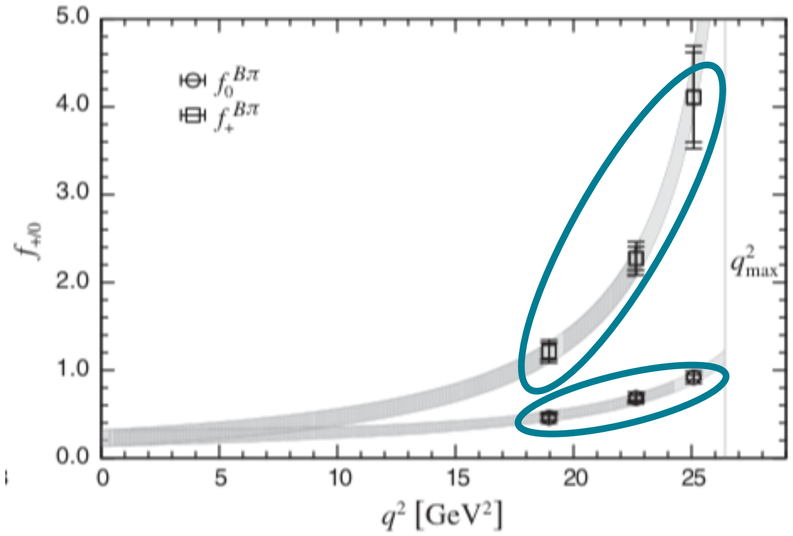

RBC/UKQCD PRD 91, 074510 (2015)

Form-factor parameterisation

$$f_X(q_i^2) = \frac{1}{B_X(q_i^2)\phi_X(q_i^2, t_0)} \sum_{n=0}^{K_X-1} a_{X,n} z(q_i^2)^n$$

unitarity constraint: $|\mathbf{a}_X|^2 \leq 1$

Boyd, Grinstein, Lebed, PRL 74 (1995)

Determine all $a_{X,n}$ from finite set of theory data

Frequentist fit:
- $N_{\text{dof}} = N_{\text{data}} - K_X \geq 1$
  $\rightarrow$ in practice truncation K at low order
- induced systematic difficult to estimate
- meaning of Frequentist with unitarity constraint?

Bayesian fit:
- fit including higher order z expansion meaningful
- unitarity regulates and controls higher-order coefficients [Flynn, AJ, Tsang JHEP 12 (2023) 175]
- well-defined meaning of unitarity constraint

Recommendation: Combined Frequentist + Bayesian perspective

BGL — conventions

$$f_X(q_i^2) = \frac{1}{B_X(q_i^2)\phi_X(q_i^2, t_0)} \sum_{n=0}^{K_X-1} a_{X,n} z(q_i^2)^n = Z_{XX,in} a_{X,n} \qquad (Z \text{ is } N_{\text{data}} \times K_X \text{ matrix})$$

E.g. $P \to P$ transition:

Input (e.g. lattice ff): $\mathbf{f}^T = (\mathbf{f}_+^T, \mathbf{f}_0^T) = (f_+(q_0^2), f_+(q_1^2), \ldots, f_+(q_{N_+-1}^2), f_0(q_0^2), f_0(q_1^2), \ldots, f_0(q_{N_0-1}^2))$

Output (BGL params): $\mathbf{a}^T = (\mathbf{a}_+^T, \mathbf{a}_0^T) = (a_{+,0}, a_{+,1}, a_{+,2}, \ldots, a_{+,K_+-1}, a_{0,1}, \ldots, a_{0,K_0-1})$

BGL — frequentist fit with kinematical constraint

Flynn, AJ, Tsang, JHEP 12 (2023) 175

Frequentist fit $\chi^2(\mathbf{a},\mathbf{f}) = [\mathbf{f} - Z\mathbf{a}]^T C_{\mathbf{f}}^{-1} [\mathbf{f} - Z\mathbf{a}]$ $f_X(q_i^2) = Z_{XX,in} a_{X,n}$

For combined fit over $f_+(q^2)$ and $f_0(q^2)$ with constraint $f_+(0) = f_0(0)$:

$$Z = \begin{pmatrix} Z_{++} & Z_{+0} \\ Z_{0+} & Z_{00} \end{pmatrix}$$

$$a_{0,0} = B_0(0)\phi_0(0,t_0)f_+(0) - \sum_{k=1}^{K_0-1} a_{0,k} z^k(0)$$

Solution: $\mathbf{a} = \left(Z^T C_{\mathbf{f}}^{-1} Z\right)^{-1} Z C_{\mathbf{f}}^{-1} \mathbf{f}$

$$C_{\mathbf{a}} = \left(Z^T C_{\mathbf{f}}^{-1} Z\right)^{-1}$$

Bayesian form-factor fit

Flynn, AJ, Tsang, JHEP 12 (2023) 175

Compute BGL parameters as expectation values $\langle g(\mathbf{a}) \rangle = \mathcal{N} \int d\mathbf{a}\, g(\mathbf{a})\, \pi(\mathbf{a}\,|\,\mathbf{f}, C_\mathbf{f})\, \pi_\mathbf{a}$

where *probability for parameters given model and data (assume input Gaussian)*

$$\pi(\mathbf{a}\,|\,\mathbf{f}, C_\mathbf{f}) \propto \exp\left(-\frac{1}{2}\chi^2(\mathbf{a},\mathbf{f})\right) \quad \text{where} \quad \chi^2(\mathbf{a},\mathbf{f}) = [\mathbf{f} - Z\mathbf{a}]^T C_\mathbf{f}^{-1} [\mathbf{f} - Z\mathbf{a}]$$

where *prior knowledge is **only** QFT unitarity constraint (flat prior for BGL params):*

$$\pi_\mathbf{a} \propto \theta\left(1 - |\,\mathbf{a}_X|^2\right)$$

In practice MC integration: draw samples for $\mathbf{a}$ from multivariate normal distribution and drop samples not compatible with unitarity

Example 1: $B_s \to K\ell\nu$ — fit to HPQCD 14

HPQCD 14
PRD 90 (2014) 054506

HPQCD 14 – $\mathbf{a}_+$

K_+	K_0	$a_{+,0}$	$a_{+,1}$	$a_{+,2}$	p	$\chi^2/N_{\rm dof}$	$N_{\rm dof}$
2	2	0.0270(13)	-0.0792(50)	-	0.03	2.93	3
2	3	0.0273(13)	-0.0760(63)	-	0.02	4.06	2
3	2	0.0257(14)	-0.0805(50)	0.068(31)	0.15	1.89	2
3	3	0.0262(14)	-0.0727(64)	0.096(34)	0.97	0.00	1

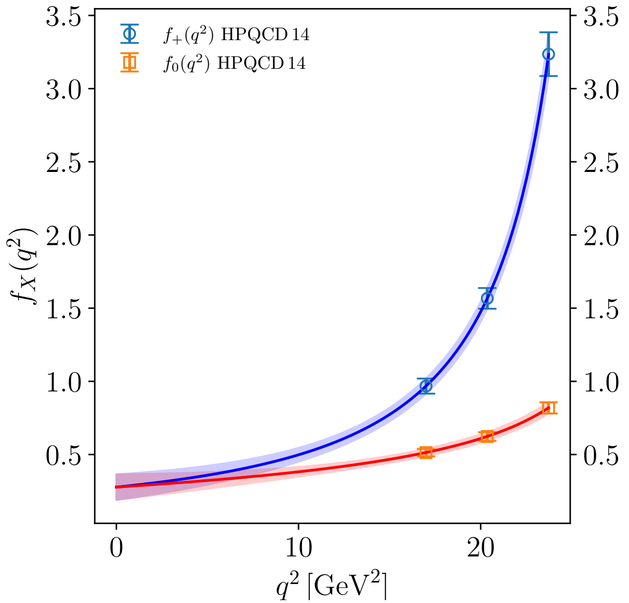

HPQCD 14 – $\mathbf{a}_0$

K_+	K_0	$a_{0,0}$	$a_{0,1}$	$a_{0,2}$	p	$\chi^2/N_{\rm dof}$	$N_{\rm dof}$
2	2	0.0883(44)	-0.250(17)	-	0.03	2.93	3
2	3	0.0880(44)	-0.242(19)	0.053(65)	0.02	4.06	2
3	2	0.0906(45)	-0.240(17)	-	0.15	1.89	2
3	3	0.0908(46)	-0.215(22)	0.138(71)	0.97	0.00	1

HPQCD 14 – $\mathbf{a}_+$ Flynn, AJ, Tsang, JHEP 12 (2023) 175

K_+	K_0	$a_{+,0}$	$a_{+,1}$	$a_{+,2}$	$a_{+,3}$	$a_{+,4}$	$a_{+,5}$	$a_{+,6}$	$a_{+,7}$	$a_{+,8}$	$a_{+,9}$
2	2	0.0270(12)	-0.0792(49)	-	-	-	-	-	-	-	-
2	3	0.0273(13)	-0.0761(63)	-	-	-	-	-	-	-	-
3	2	0.0257(14)	-0.0805(49)	0.069(30)	-	-	-	-	-	-	-
3	3	0.0261(14)	-0.0728(64)	0.096(34)	-	-	-	-	-	-	-
3	4	0.0261(14)	-0.0728(76)	0.096(39)	-	-	-	-	-	-	-
4	3	0.0261(14)	-0.0729(68)	0.096(35)	0.008(90)	-	-	-	-	-	-
4	4	0.0261(14)	-0.0730(77)	0.091(62)	-0.02(20)	-	-	-	-	-	-
5	5	0.0262(15)	-0.0735(79)	0.084(67)	-0.03(19)	0.03(68)	-	-	-	-	-
6	6	0.0261(14)	-0.0735(79)	0.086(69)	-0.03(19)	-0.00(64)	0.01(65)	-	-	-	-
7	7	0.0262(14)	-0.0732(84)	0.088(69)	-0.02(18)	0.01(65)	0.02(73)	-0.03(70)	-	-	-
8	8	0.0261(14)	-0.0732(80)	0.089(72)	-0.02(18)	-0.00(66)	0.03(86)	-0.04(90)	0.03(73)	-	-
9	9	0.0261(14)	-0.0729(84)	0.095(75)	-0.02(19)	-0.04(68)	0.1(1.0)	-0.1(1.2)	0.1(1.1)	-0.06(79)	-
10	10	0.0261(14)	-0.0726(89)	0.101(79)	-0.01(20)	-0.09(73)	0.2(1.3)	-0.3(1.7)	0.2(1.8)	-0.2(1.4)	0.08(87)

results stable as truncation relaxed

HPQCD 14 – $\mathbf{a}_0$

K_+	K_0	$a_{0,0}$	$a_{0,1}$	$a_{0,2}$	$a_{0,3}$	$a_{0,4}$	$a_{0,5}$	$a_{0,6}$	$a_{0,7}$	$a_{0,8}$	$a_{0,9}$
2	2	0.0883(44)	-0.250(17)	-	-	-	-	-	-	-	-
2	3	0.0880(44)	-0.243(19)	0.052(65)	-	-	-	-	-	-	-
3	2	0.0907(46)	-0.240(17)	-	-	-	-	-	-	-	-
3	3	0.0906(44)	-0.215(22)	0.137(73)	-	-	-	-	-	-	-
3	4	0.0907(47)	-0.215(22)	0.14(11)	-0.01(31)	-	-	-	-	-	-
4	3	0.0907(45)	-0.214(22)	0.139(72)	-	-	-	-	-	-	-
4	4	0.0907(46)	-0.215(25)	0.12(19)	-0.08(60)	-	-	-	-	-	-
5	5	0.0909(46)	-0.218(25)	0.10(19)	-0.12(55)	0.04(63)	-	-	-	-	-
6	6	0.0907(45)	-0.217(25)	0.10(19)	-0.11(53)	0.06(66)	-0.02(66)	-	-	-	-
7	7	0.0907(46)	-0.217(26)	0.11(20)	-0.08(51)	0.03(73)	0.03(81)	-0.04(70)	-	-	-
8	8	0.0908(46)	-0.217(25)	0.11(20)	-0.08(50)	-0.01(84)	0.1(1.0)	-0.09(96)	0.08(74)	-	-
9	9	0.0907(46)	-0.215(25)	0.13(22)	-0.05(50)	-0.06(95)	0.2(1.4)	-0.2(1.5)	0.1(1.2)	-0.05(82)	-
10	10	0.0907(46)	-0.214(27)	0.15(24)	-0.03(49)	-0.2(1.1)	0.4(1.8)	-0.5(2.2)	0.4(2.1)	-0.3(1.6)	0.13(90)

Example 1: $B_s \to K\ell\nu$ — fit to HPQCD 14

results for phenomenology in Bayesian setup independent of truncation

increasing truncation

Results for HPQCD 14 PRD 90 (2014) 054506

Flynn, AJ, Tsang, JHEP 12 (2023) 175

K_+	K_0	$f(q^2=0)$	$R^{\rm impr}_{B_s\to K}$	$R_{B_s\to K}$	$\frac{\Gamma^\tau}{\lvert V_{ub}\rvert^2}\,[\frac{1}{\rm ps}]$	$\frac{\Gamma^\mu}{\lvert V_{ub}\rvert^2}\,[\frac{1}{\rm ps}]$	$V^{\rm low}_{\rm CKM}$	$V^{\rm high}_{\rm CKM}$	$V^{\rm full}_{\rm CKM}$
2	2	0.208(25)	1.524(37)	0.727(25)	4.51(45)	6.23(76)	0.00383(47)	0.00352(35)	0.00363(37)
2	3	0.226(34)	1.511(41)	0.704(39)	4.67(49)	6.67(97)	0.00361(53)	0.00344(34)	0.00349(38)
3	2	0.233(27)	1.609(58)	0.733(27)	4.44(45)	6.08(77)	0.00368(45)	0.00367(37)	0.00367(38)
3	3	0.293(41)	1.592(57)	0.664(40)	4.84(51)	7.3(1.1)	0.00310(44)	0.00349(35)	0.00333(36)
3	4	0.293(56)	1.593(60)	0.667(59)	4.85(58)	7.4(1.4)	0.00313(55)	0.00349(37)	0.00338(40)
4	3	0.294(42)	1.594(60)	0.663(40)	4.85(52)	7.4(1.1)	0.00309(44)	0.00348(36)	0.00332(36)
4	4	0.285(92)	1.593(60)	0.677(88)	4.83(62)	7.3(1.7)	0.00328(86)	0.00350(38)	0.00346(42)
5	5	0.277(88)	1.595(62)	0.685(85)	4.81(62)	7.2(1.7)	0.00333(85)	0.00351(38)	0.00348(42)
6	6	0.277(88)	1.592(63)	0.685(86)	4.79(63)	7.2(1.7)	0.00335(88)	0.00350(38)	0.00348(43)
7	7	0.282(89)	1.592(60)	0.680(87)	4.82(64)	7.3(1.7)	0.00332(89)	0.00350(38)	0.00347(43)
8	8	0.283(88)	1.594(61)	0.679(85)	4.83(64)	7.3(1.7)	0.00330(85)	0.00351(37)	0.00347(41)
9	9	0.289(91)	1.594(62)	0.674(88)	4.85(64)	7.4(1.8)	0.00327(89)	0.00350(38)	0.00347(42)
10	10	0.293(95)	1.593(60)	0.670(91)	4.87(67)	7.5(1.9)	0.00325(92)	0.00349(38)	0.00346(42)

increasing truncation

K_+	K_0	$I[\mathcal{A}^\tau_{\rm FB}]\,[\frac{1}{\rm ps}]$	$I[\mathcal{A}^\mu_{\rm FB}]\,[\frac{1}{\rm ps}]$	$\bar{\mathcal{A}}^\tau_{\rm FB}$	$\bar{\mathcal{A}}^\mu_{\rm FB}$	$I[\mathcal{A}^\tau_{\rm pol}]\,[\frac{1}{\rm ps}]$	$I[\mathcal{A}^\mu_{\rm pol}]\,[\frac{1}{\rm ps}]$	$\bar{\mathcal{A}}^\tau_{\rm pol}$	$\bar{\mathcal{A}}^\mu_{\rm pol}$
2	2	1.22(13)	0.0278(51)	0.2708(37)	0.00443(34)	0.74(15)	6.15(75)	0.164(29)	0.98767(96)
2	3	1.26(14)	0.0314(70)	0.2709(38)	0.00465(44)	0.81(18)	6.59(96)	0.173(31)	0.9872(12)
3	2	1.23(13)	0.0319(59)	0.2780(43)	0.00524(51)	0.46(19)	5.99(76)	0.103(40)	0.9852(15)
3	3	1.36(15)	0.045(10)	0.2814(48)	0.00612(66)	0.53(20)	7.2(1.1)	0.110(40)	0.9830(18)
3	4	1.37(17)	0.046(14)	0.2814(50)	0.00611(83)	0.53(22)	7.3(1.3)	0.109(41)	0.9830(22)
4	3	1.37(15)	0.046(10)	0.2815(50)	0.00616(71)	0.53(22)	7.2(1.1)	0.109(42)	0.9829(20)
4	4	1.36(19)	0.046(21)	0.2810(69)	0.0060(15)	0.53(21)	7.2(1.7)	0.109(42)	0.9834(41)
5	5	1.35(19)	0.044(20)	0.2806(67)	0.0058(15)	0.53(22)	7.1(1.6)	0.109(44)	0.9837(39)
6	6	1.35(20)	0.044(20)	0.2803(69)	0.0058(15)	0.53(22)	7.1(1.7)	0.111(44)	0.9838(39)
7	7	1.35(20)	0.045(20)	0.2806(69)	0.0059(15)	0.53(21)	7.2(1.7)	0.111(43)	0.9835(39)
8	8	1.36(20)	0.045(20)	0.2808(69)	0.0059(15)	0.53(22)	7.2(1.7)	0.109(44)	0.9835(39)
9	9	1.36(20)	0.047(21)	0.2812(71)	0.0060(15)	0.53(22)	7.3(1.7)	0.109(44)	0.9832(40)
10	10	1.37(21)	0.048(23)	0.2815(72)	0.0061(15)	0.53(22)	7.4(1.8)	0.109(43)	0.9831(41)

Example 1: $B_s \to K\ell\nu$ — global fit

Combined fit over three lattice data sets — let's first look at **Frequentist**:

[HPQCD 14 PRD 90 (2014), RBC/UKQCD 23 PRD 107 (2023) FNAL/MILC 19 PRD 100 (2019)]

K_+	K_0	$a_{+,0}$	$a_{+,1}$	$a_{+,2}$	$a_{+,3}$	$a_{+,4}$	p	$\chi^2/N_{\rm dof}$	$N_{\rm dof}$
2	2	0.02641(58)	-0.0824(26)	-	-	-	0.00	5.15	14
2	3	0.02668(68)	-0.0811(31)	-	-	-	0.00	5.50	13
3	2	0.02477(68)	-0.0829(26)	0.054(12)	-	-	0.00	3.95	13
3	3	0.02534(73)	-0.0792(31)	0.062(12)	-	-	0.00	3.89	12
3	4	0.02534(73)	-0.0781(34)	0.067(14)	-	-	0.00	4.19	11
4	3	0.02535(73)	-0.0776(38)	0.074(20)	0.023(30)	-	0.00	4.19	11
4	4	0.02592(97)	-0.033(50)	0.69(69)	2.1(2.3)	-	0.00	4.53	10
5	5	0.0266(10)	0.052(65)	2.21(97)	11.1(5.6)	17.2(15.1)	0.00	5.04	8

K_+	K_0	$a_{0,0}$	$a_{0,1}$	$a_{0,2}$	$a_{0,3}$	$a_{0,4}$	p	$\chi^2/N_{\rm dof}$	$N_{\rm dof}$
2	2	0.0854(17)	-0.2565(75)	-	-	-	0.00	5.15	14
2	3	0.0856(18)	-0.2527(91)	0.021(27)	-	-	0.00	5.50	13
3	2	0.0858(18)	-0.2501(77)	-	-	-	0.00	3.95	13
3	3	0.0864(18)	-0.2379(95)	0.061(28)	-	-	0.00	3.89	12
3	4	0.0869(19)	-0.231(13)	0.067(29)	-0.08(10)	-	0.00	4.19	11
4	3	0.0869(19)	-0.229(15)	0.091(48)	-	-	0.00	4.19	11
4	4	0.0887(27)	-0.08(17)	2.2(2.4)	7.0(7.9)	-	0.00	4.53	10
5	5	0.0887(28)	0.07(20)	6.1(3.3)	41.5(19.0)	93.3(44.0)	0.00	5.04	8

Bayesian fit works but doesn't describe data:

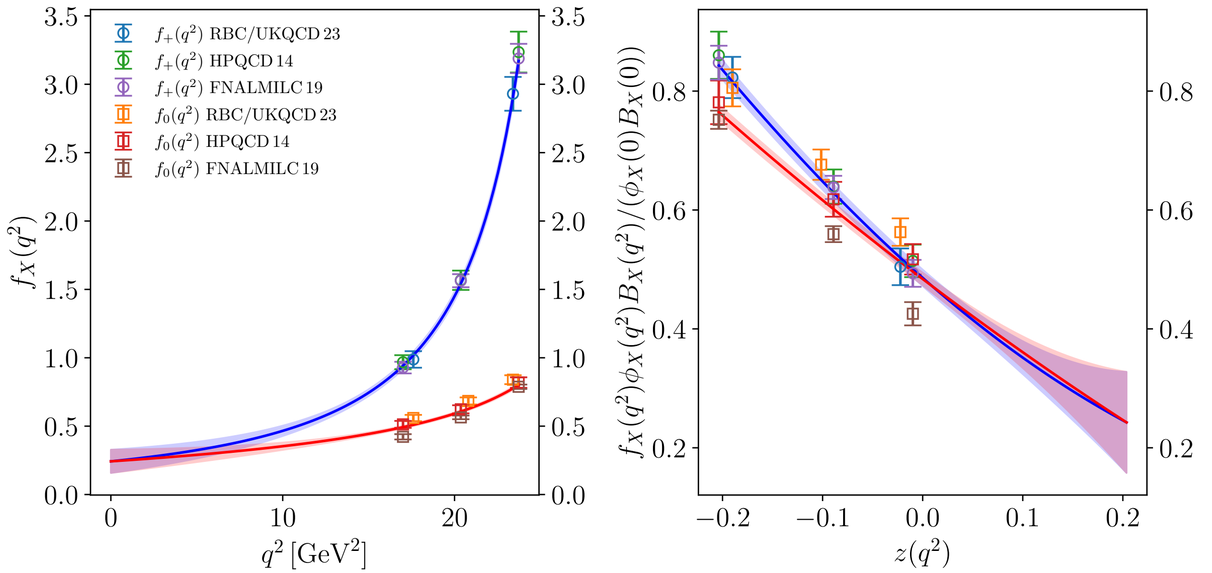

In the case at hand: World lattice data for $B_s \to K\ell\nu$ requires further scrutiny; Frequentist fit indicates problem!

[see for possible explanation RBC/UKQCD 23 PRD 107 (2023)]

Bayesian and frequentist provide complementary information — use both to gain comprehensive understanding of data and fit

Example 2: $B \to \pi l \nu$ and $B_s \to K l \nu$

Idea: simultaneous Bayesian fit over both channels subject to combined unitarity constraint

dispersion relation

$$\chi_X \geq \int_{t_{B\pi}}^{\infty} dt \frac{W_{B\pi}(t)\,|f_X^{B\to\pi}(t)|^2}{(t-q^2)^{n_X}} + \int_{t_{B_sK}}^{\infty} dt \frac{W_{B_sK}(t)\,|f_X^{B_s\to K}(t)|^2}{(t-q^2)^{n_X}} \quad \to \quad 1 \geq |\vec{a}_X^{B\to\pi}|^2 + |\vec{a}_X^{B_s\to K}|^2 \qquad (X = +, 0)$$

Lattice data: $B_s \to K$ [HPQCD 14 PRD 90 (2014), RBC/UKQCD 23 PRD 107 (2023)]

$B \to \pi$ [JLQCD 22 PRD 106 (2022)]

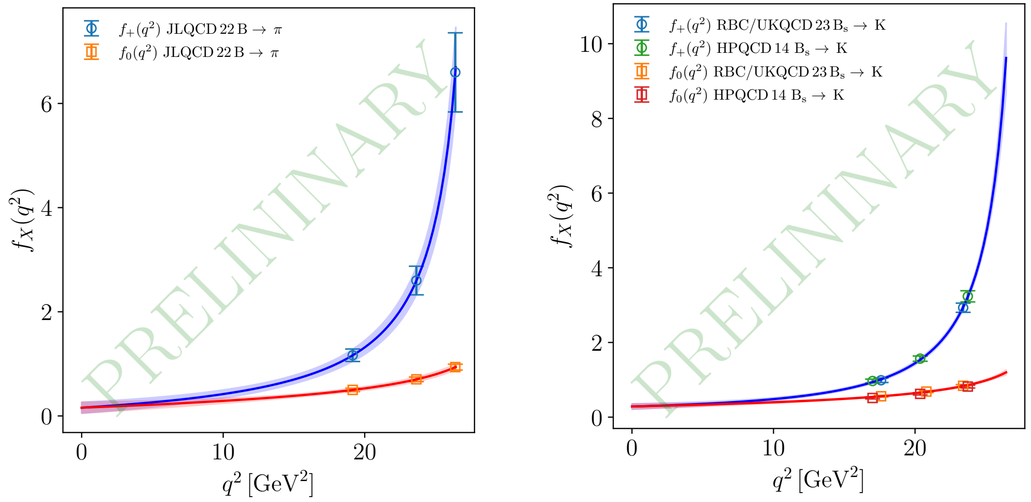

- we find simultaneous unitarity constraint stronger than individual
- effect will depend on channel
- in case at hand coefficients have noticeably smaller error
- work in progress

Relation to dispersive-matrix method?

Di Carlo, Martinelli, Naviglio et al. PRD 104 (2021) 054502

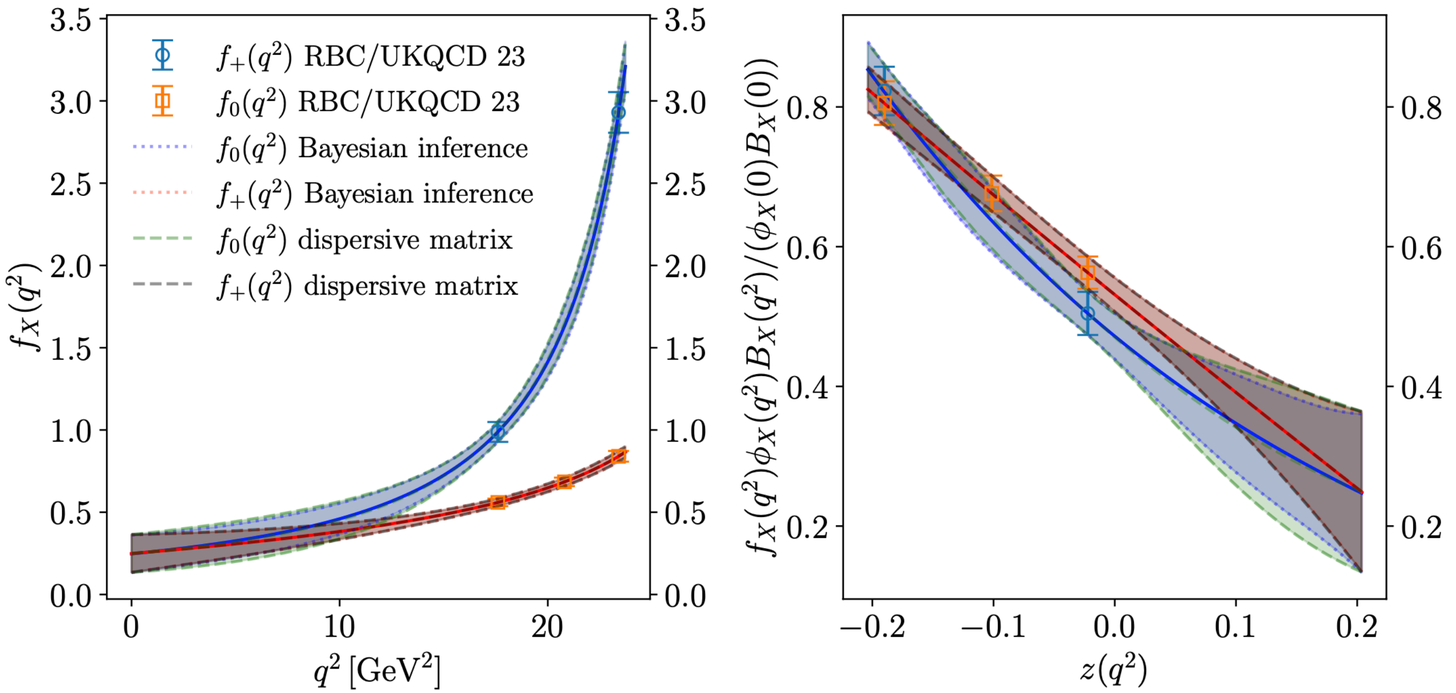

The methods produce essentially the same results. Clear practical advantages of Bayesian inference:

- kinematical constraints exactly and cleanly implemented
- simultaneous fit over various (correlated) data sets possible
- clean statistical underpinning

$$B \to D^{*} \ell \bar{\nu}$$

A small tension…

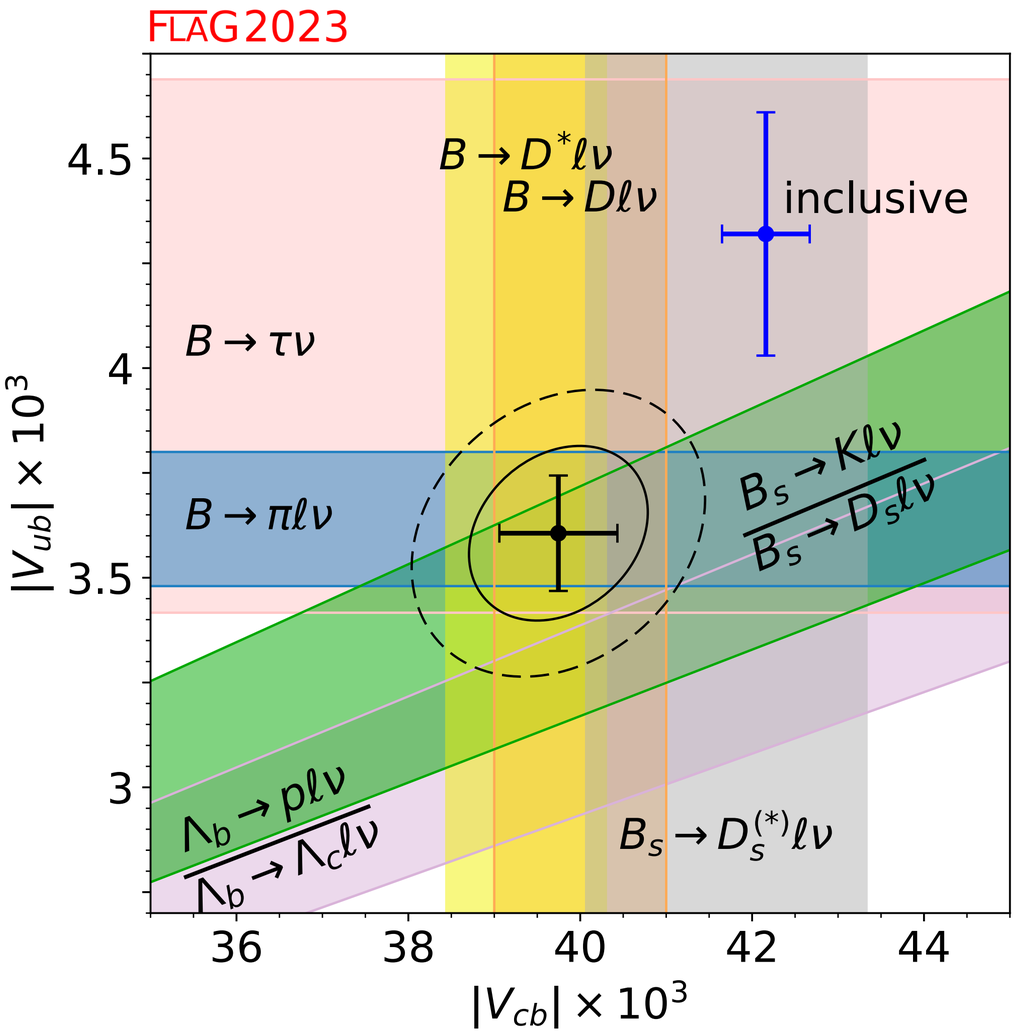

Various ways to look at the $|V_{cb}|$ tension

A) Exclusive decay $B \to D^* \ell \bar{\nu}_\ell$:
- new quality of experimental data
- new quality of lattice data

→ discuss new and improved analysis techniques

B) Inclusive decay $B \to X_c \ell \bar{\nu}_\ell$:
- existing determinations OPE based
- new ideas allow for lattice computations

→ happy to discuss

Hansen et al. (2017) PRD 96 094513 (2017)
Hashimoto PTEP 53-56 (2017)
Bailas et al. PTEP 43-50 (2020)
Barone et al. JHEP 07 (2023) 145
Ryan's talk on Wednesday

New lattice data — $B \to D^* \ell \bar{\nu}_\ell$

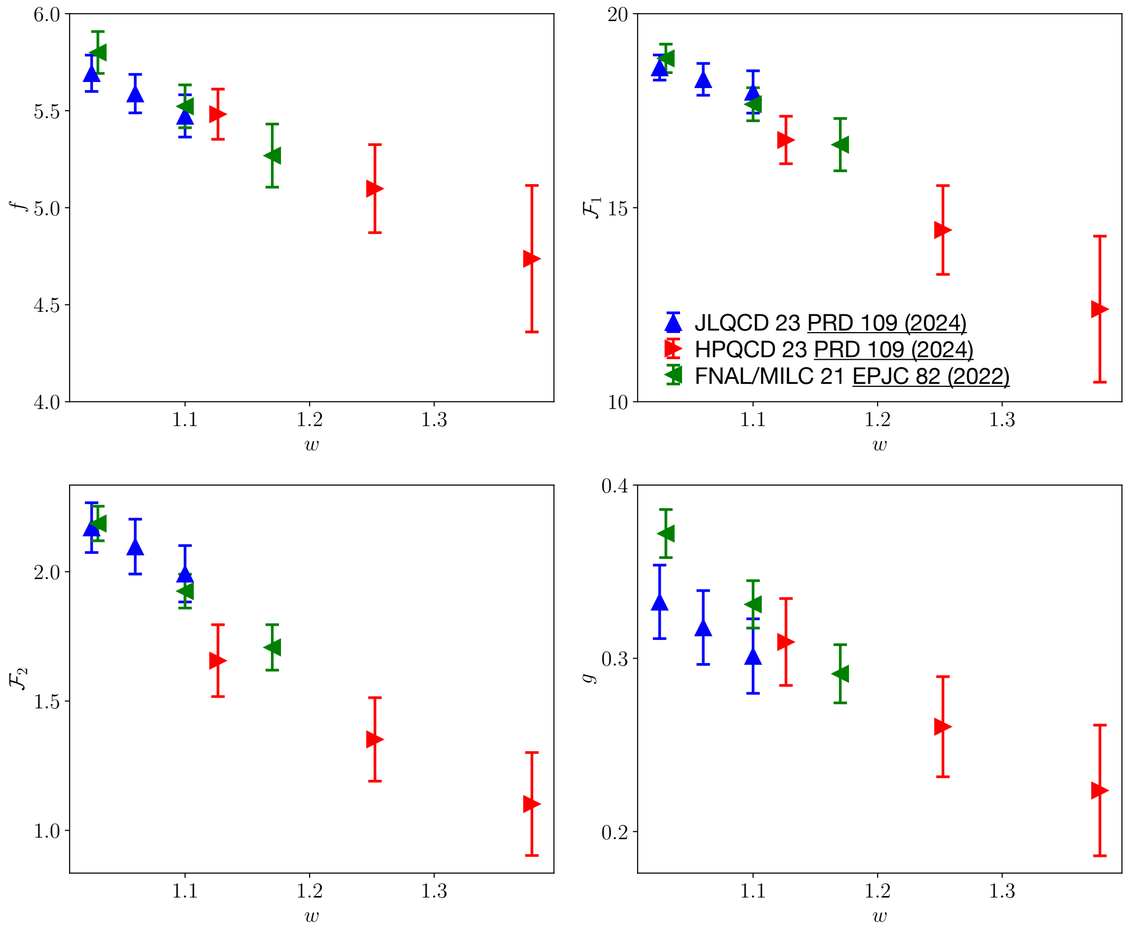

New lattice data

- four form factors $f, \mathcal{F}_1, \mathcal{F}_2, g$

$$w = \frac{M_B^2 + M_{D^*}^2 - q^2}{2 M_B M_{D^*}} \qquad q_\mu = (p_B - p_{D^*})_\mu$$

- first time that lattice data covers kinematical range
- three different and independent collaborations
- just in time for new experimental data ...

New experimental data — $B \to D^* \ell \bar{\nu}_\ell$

Belle Phys.Rev.D 108 (2023) 1, 012002
Belle II Phys.Rev.D 108 (2023) 9, 9

Thanks to HFLAV for combined data set (in particular Florian Bernlochner and Markus Prim)

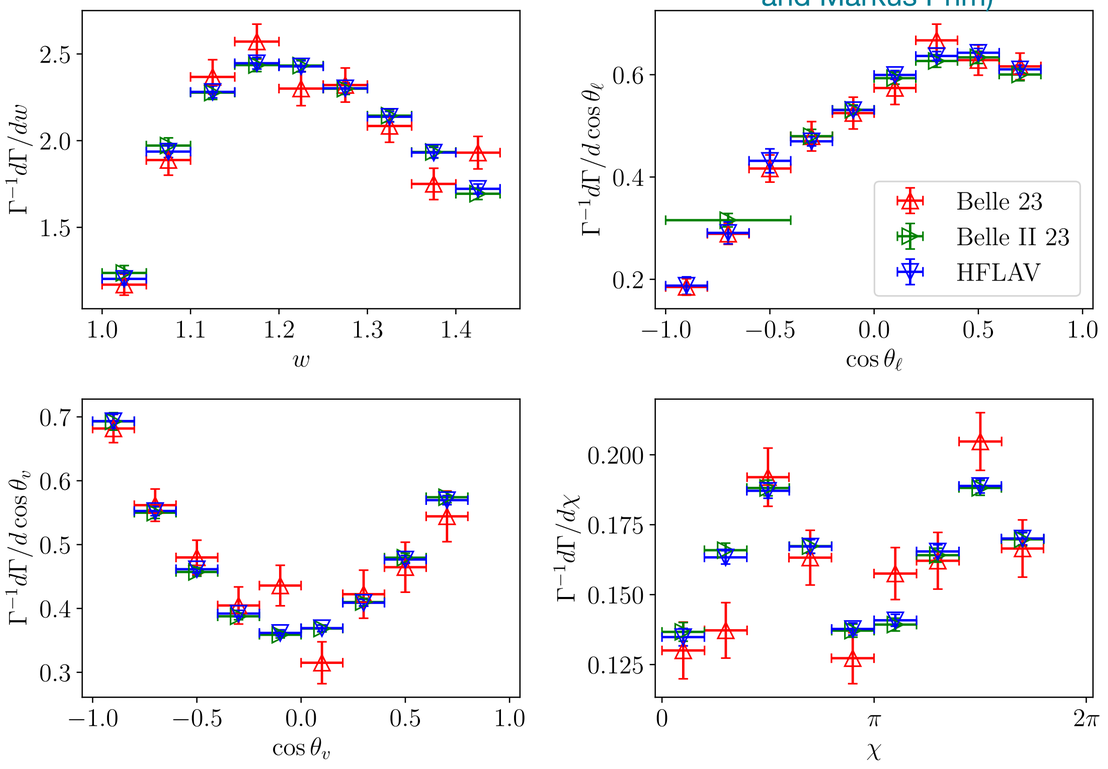

here not Belle 2310.20286 (angular coeffs)

New experimental data

- four (normalised) differential decay rates in channels

$$\alpha = w,\ \cos\theta_\ell,\ \cos\theta_v, \chi$$

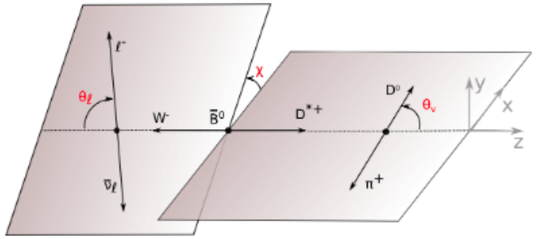

- between 7 and 10 bins per α
- data available on HEPData
- two experimental collaborations
- just in time for new lattice data …

$$\begin{aligned}\frac{d\Gamma}{dw d\cos(\theta_\ell) d\cos(\theta_v) d\chi} = &\frac{3G_F^2}{1024\pi^4}|V_{cb}|^2 \eta_{EW}^2 M_B r^2 \sqrt{w^2-1} q^2 \\ &\times \{(1-\cos(\theta_\ell))^2 \sin^2(\theta_v) H_+^2(w) + (1+\cos(\theta_\ell))^2 \sin^2(\theta_v) H_-^2(w) \\ &+ 4\sin^2(\theta_\ell)\cos^2(\theta_v) H_0^2(w) - 2\sin^2(\theta_\ell)\sin^2(\theta_v)\cos(2\chi) H_+(w) H_-(w) \\ &- 4\sin(\theta_\ell)(1-\cos(\theta_\ell))\sin(\theta_v)\cos(\theta_v)\cos(\chi) H_+(w) H_0(w) \\ &+ 4\sin(\theta_\ell)(1+\cos(\theta_\ell))\sin(\theta_v)\cos(\theta_v)\cos(\chi) H_-(w) H_0(w)\}\end{aligned}$$

How to best analyse this new quality of data as part of a precision test of the SM?

Fitting strategies

A

- fit parameterisation to lattice data
- compute theory prediction for $d\Gamma/dq^2/|V_{cb}|^2$ bin-by-bin by integration
- combine with experimental data for bin-by-bin prediction for $|V_{cb}|$
- final $|V_{cb}|$ from weighted average over bins

Clean separation of SM and exp. measurement

B

- fit parameterisation simultaneously to lattice form factors and results for experimental data for diff. decay rate (use shape-information from both experiment and lattice)
- determine $|V_{cb}|$ directly from such a global fit

Unitarity constraint and fit-ansatz imposed on experimental data (which may contain BSM)

Here concentrate on:
Flynn, AJ, Tsang JHEP 12 (2023)
Bordone, AJ 2406.10074

Other related work:
Fedele et al. PRD 108 (2023) 5, 5
Martinelli et al. EPJC 84 (2024) 4, 400,
PRD 106 (2022) 9, 093002,
EPJC 82 (2022) 12,
PRD 105 (2022) 3, 034503,
PRD 104 (2021) 9, 094512
Di Carlo et al. PRD 104 (2021) 5, 054502
Gambino PLB 795 (2019) 386-390
Bigi PLB 769 (2017) 441-445, JHEP 11 (2017) 061
Bernlochner et al. PRD 100 (2019) 1, 013005

SM correct — A and B should result in compatible predictions

Strategy A: Fit to lattice data

Bordone, AJ, 2406.10074

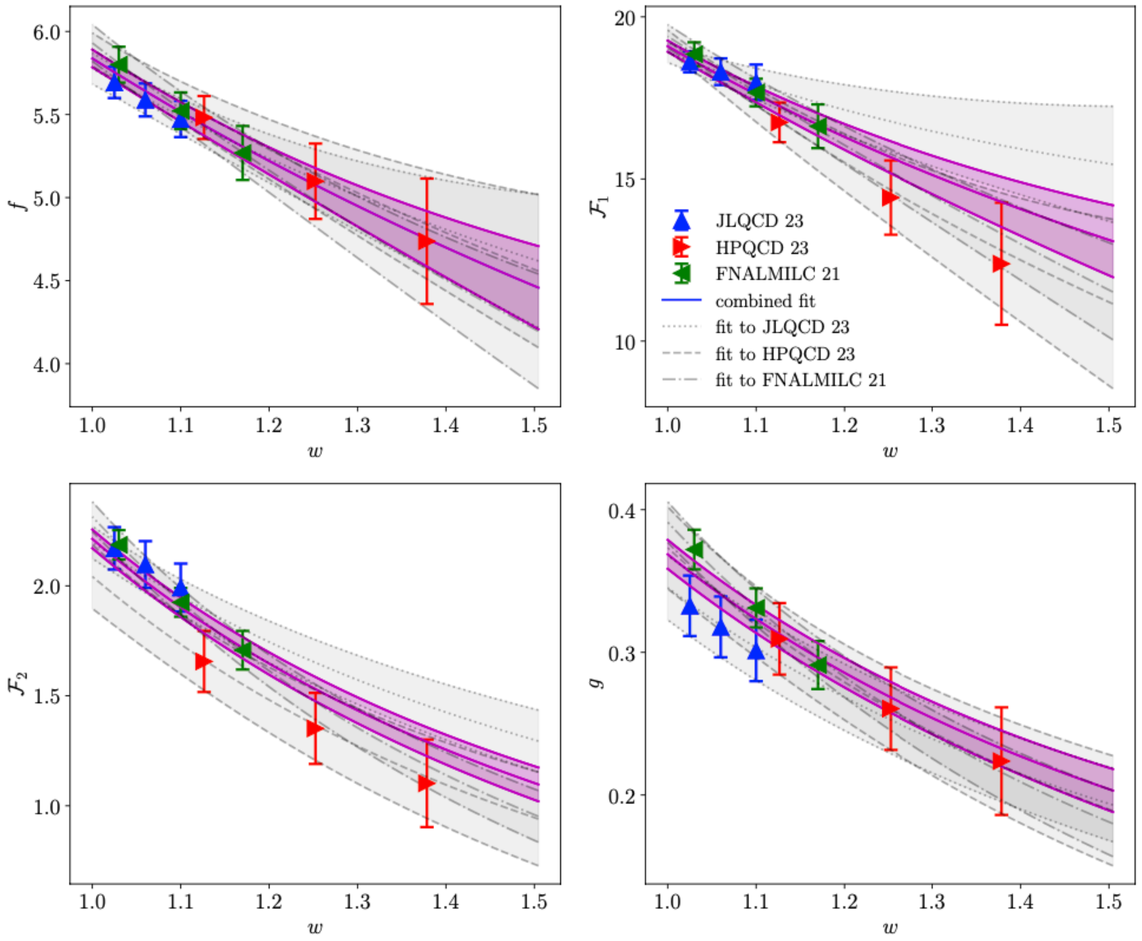

Frequentist fit

K_f	K_{F_1}	K_{F_2}	K_g	$a_{g,0}$	$a_{g,1}$	$a_{g,2}$	$a_{g,3}$	p	$\chi^2/N_{\rm dof}$	$N_{\rm dof}$
2	2	2	2	0.03138(87)	-0.059(24)	-	-	0.95	0.62	30
3	3	3	3	0.03131(87)	-0.046(36)	-1.2(1.8)	-	0.90	0.67	26
4	4	4	4	0.03126(87)	-0.017(48)	-3.7(3.3)	49.9(53.6)	0.79	0.75	22

- good fit quality
- lattice data compatible
- no unitarity constraint

Bayesian inference

K_f	K_{F_1}	K_{F_2}	K_g	$a_{g,0}$	$a_{g,1}$	$a_{g,2}$	$a_{g,3}$
2	2	2	2	0.03133(80)	-0.058(25)	-	-
3	3	3	3	0.03129(81)	-0.062(27)	-0.10(55)	-
4	4	4	4	0.03134(86)	-0.061(25)	-0.10(50)	-0.04(49)

- unitarity constraint regulates higher-order coefficients
- truncation independent

Strategy B: Fit to lattice + exp.data

Bordone, AJ, 2406.10074

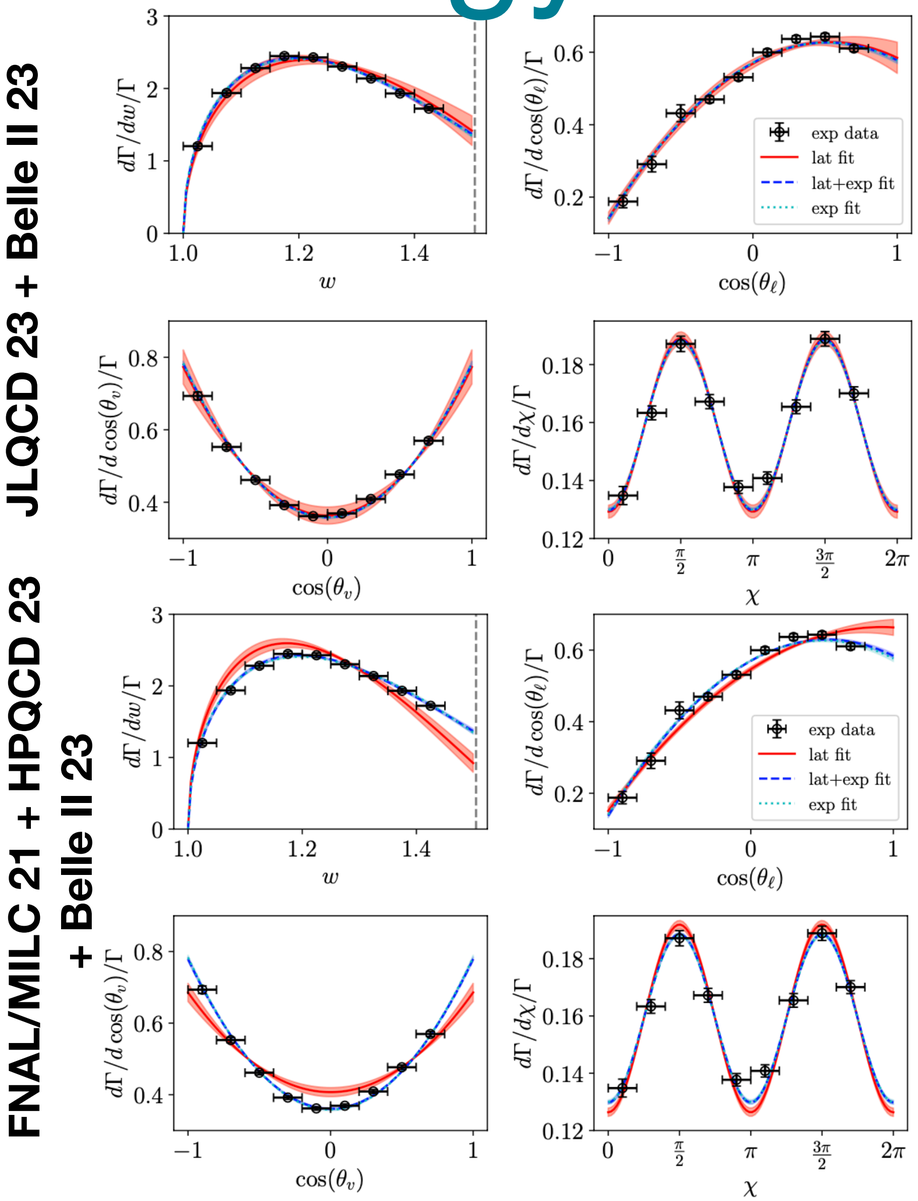

- BGL fit to only lattice data (strategy A) misses experimental points for two of the lattice data sets
- BGL fit to experimental and lattice data of good quality

  Frequentist fit quality good

  lat $(p, \chi^2/N_{\rm dof}, N_{\rm dof}) = (0.79, 0.75, 22)$

  lat+exp $(p, \chi^2/N_{\rm dof}, N_{\rm dof}) = (0.18, 1.15, 56)$

- some BGL coefficients shift between strategy A) and B) by up to a few $\sigma \rightarrow$ but precision of lattice data allows for enough wiggle room

Strategy B: Fit to lattice + experimental data

Bordone, AJ, 2406.10074

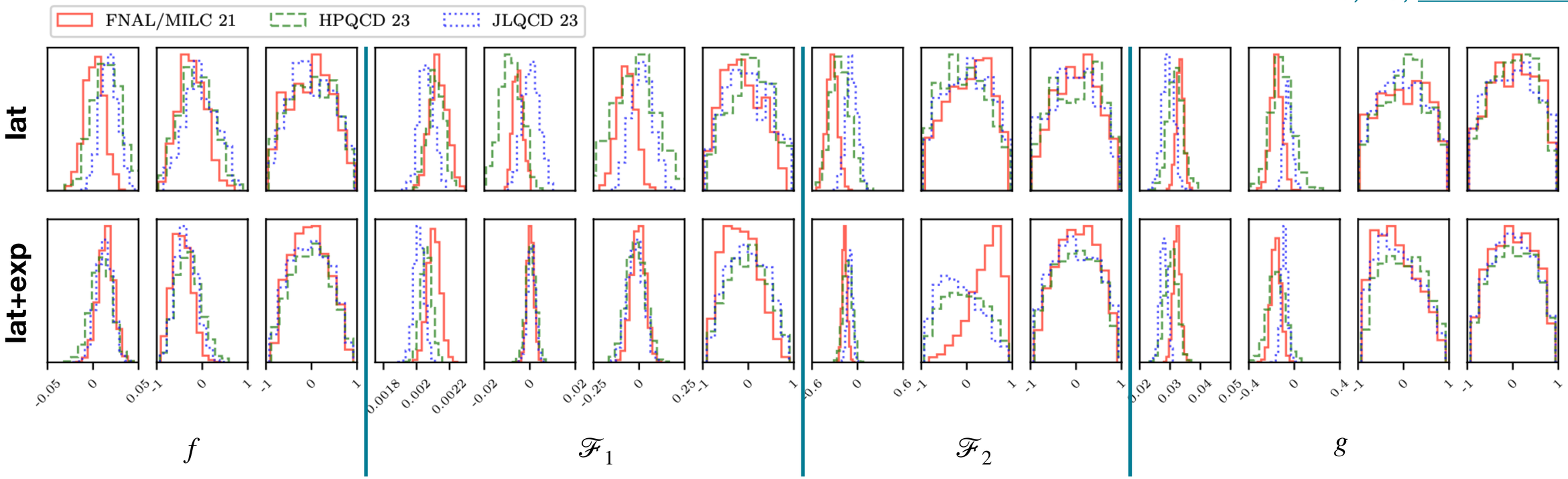

- posterior distribution reflect small shifts between lat and lat+exp fits
- higher-order coefficients “regulated” by unitarity constraint
- strange behaviour in $a_{\mathcal{F}_{2,2}}$ for FNAL/MILC-based fit?

Other observables

Bordone, AJ, 2406.10074

e.g. Forward-Backward asymmetry

$$A_{\rm FB} = \frac{\int_0^1 - \int_{-1}^0 d\cos\theta_\ell d\Gamma/d\cos\theta_\ell}{\int_0^1 + \int_{-1}^0 d\cos\theta_\ell d\Gamma/d\cos\theta_\ell}$$

JLQCD 23 + Belle II 23

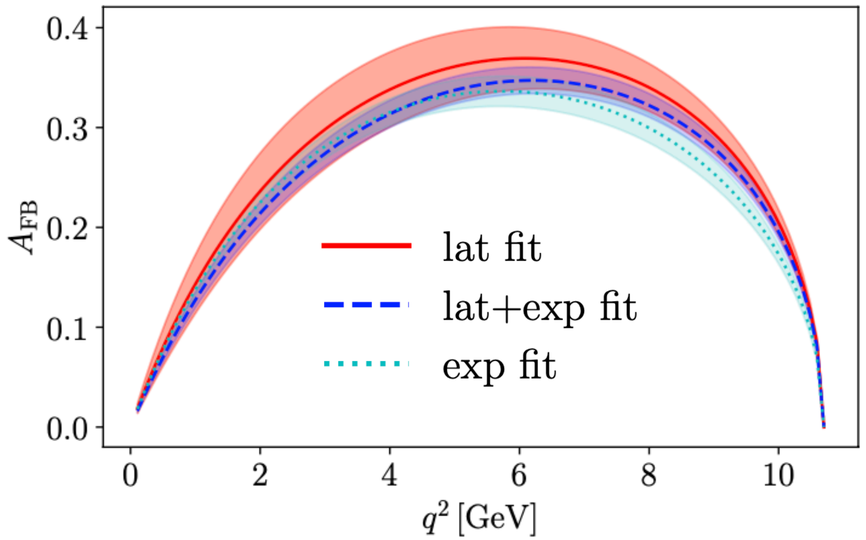

FNAL/MILC 21 + HPQCD 23 + Belle II 23

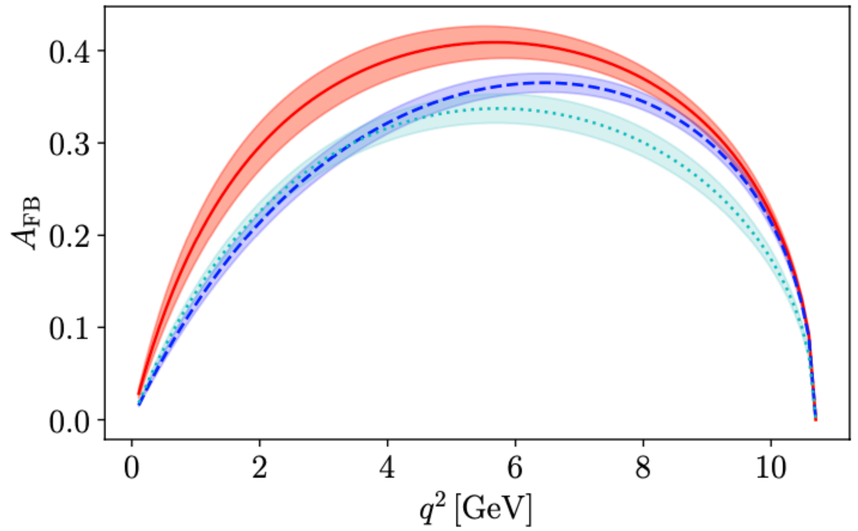

precision of lat and exp data allow to identify differences in shapes of distributions
Here: lat, lat+exp and exp parameterisations exhibit distinctly different shapes

Other observables

Bordone, AJ, 2406.10074

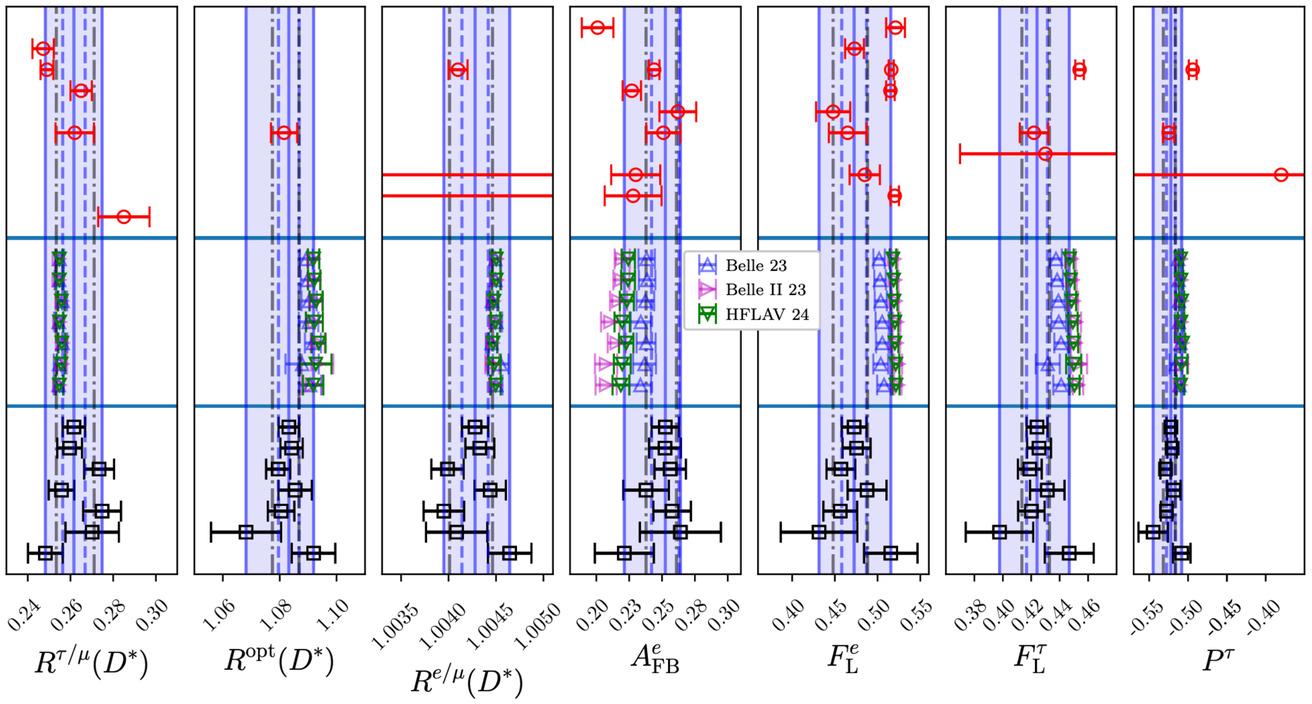

Bobeth et al. [71]
Bordone et al. [70]
Bernlochner et al. [23]
dispersive matrix Fedele et al. "lat+exp" [34]
dispersive matrix Fedele et al. "lat" [34]
dispersive matrix Martinelli et al. [33]
LHCb [69]
Belle [1, 67, 68]
Belle II [3, 66]
HFLAV Moriond 2024 (exp. average) [65]

exp+lat: JLQCD 23, HPQCD 23, FNALMILC 21
exp+lat: JLQCD 23, FNALMILC 21
exp+lat: FNALMILC 21, HPQCD 23
exp+lat: JLQCD 23, HPQCD 23
exp+lat: FNALMILC 21
exp+lat: HPQCD 23
exp+lat: JLQCD 23

lat: JLQCD 23, HPQCD 23, FNALMILC 21
lat: JLQCD 23, FNALMILC 21
lat: FNALMILC 21, HPQCD 23
lat: JLQCD 23, HPQCD 23
lat: FNALMILC 21
lat: HPQCD 23
lat: JLQCD 23

$R^{\rm opt}$ see Isidori, Sumensari, EPJC 80 (2020) 11, 1078]

- lat: scatter from different lattice collaborations concerning (2-3σ) (see also [Fedele et al. PRD 108, 055037 (2023)])
- lat+exp: lattice consistent, experiments inconsistent
- parameterisation-based observables show high degree of sensitivity

analysis reveals tensions amongst lattice as well as amongst experimental data sets

$|V_{cb}|$ — Strategy A: Fit to lattice data

Bordone, AJ, 2406.10074

$$|V_{cb}|_{\alpha,i} = \left(\Gamma_{\rm exp} \left[\frac{1}{\Gamma} \frac{d\Gamma}{d\alpha} \right]^{(i)}_{\rm exp} \Big/ \left[\frac{d\Gamma_0}{d\alpha}(\mathbf{a}) \right]^{(i)}_{\rm lat} \right)^{1/2}, \qquad \text{where} \qquad \Gamma_{\rm exp} = \frac{\mathcal{B}(B^0 \to D^{*,-}\ell^+\nu_\ell)}{\tau(B^0)},$$

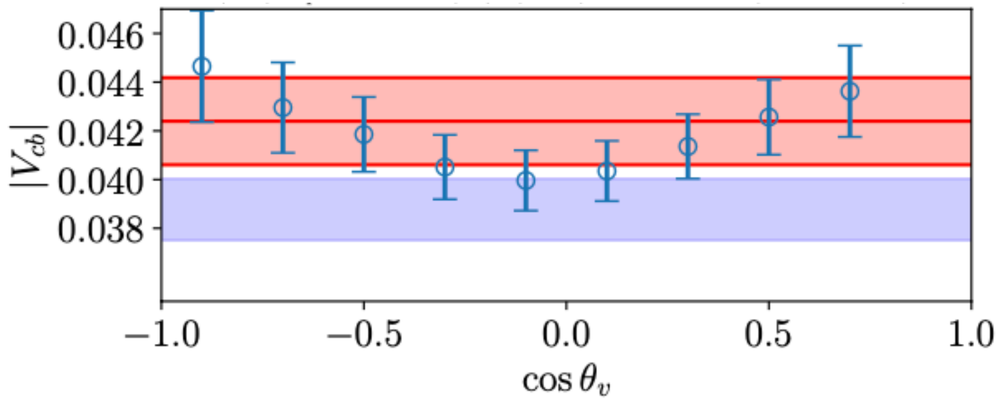

blue:
- Frequentist fit $(p, \chi^2/N_{\rm dof}, N_{\rm dof}) = (0.00, 2.82, 8)$
- d'Agostini Bias? [d'Agostini, Nucl.Instrum.Meth.A 346 (1994)]

red:
- Akaike-Information-Criterion analysis [H. Akaike IEEE TAC (19,6,1974)] average over all possible fits with at least two data points and then weighted average:

$$w_{\{\alpha,i\}} = \mathcal{N}^{-1} \exp\left(-\frac{1}{2}(\chi^2_{\{\alpha,i\}} - 2N_{{\rm dof},\{\alpha,i\}}) \right) \qquad \mathcal{N} = \sum_{{\rm set}\in\{\alpha,i\}} w_{\rm set}$$

$$|V_{cb}| = \langle |V_{cb}| \rangle \equiv \sum_{{\rm set}\in\{\alpha,i\}} w_{\rm set} |V_{cb}|_{\rm set}$$

- result more *sensible* and bias apparently reduced

$|V_{cb}|$ — Strategy A: different lattice input — different

Bordone, AJ, 2406.10074

JLQCD 23

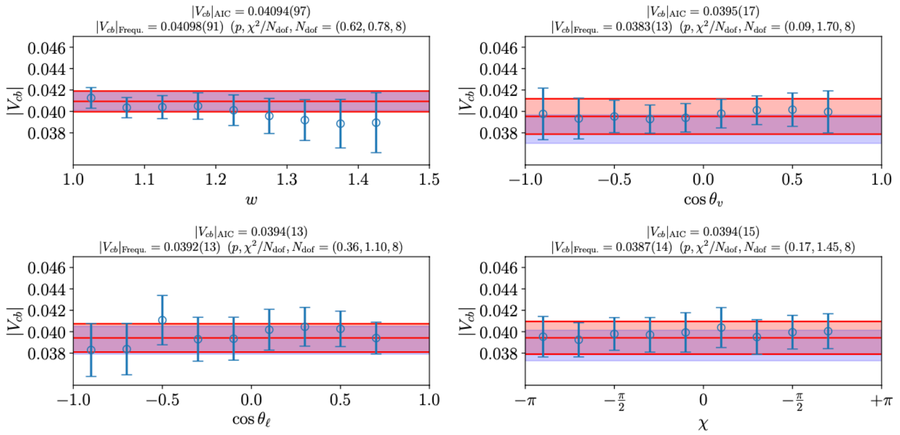

HPQCD 23

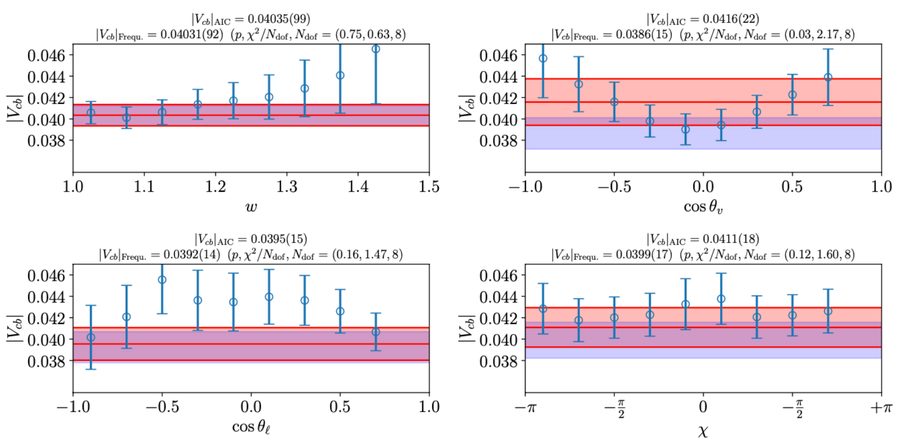

FNAL/MILC 21

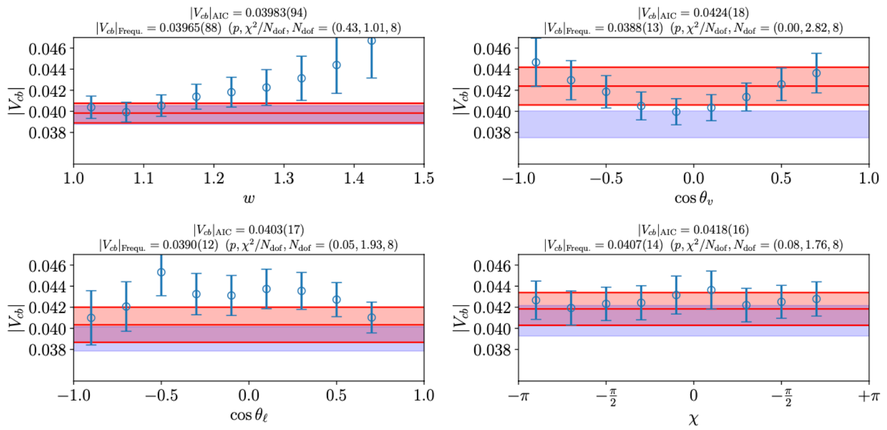

- AIC approach works nicely
- some lattice data however problematic and at odds with expectation
- in particular analysis of angular distributions problematic?
- discard analysis $X = \cos\theta_v,\ \cos\theta_\ell, \chi$?

$|V_{cb}|$ – Summary

Bordone, AJ, 2406.10074

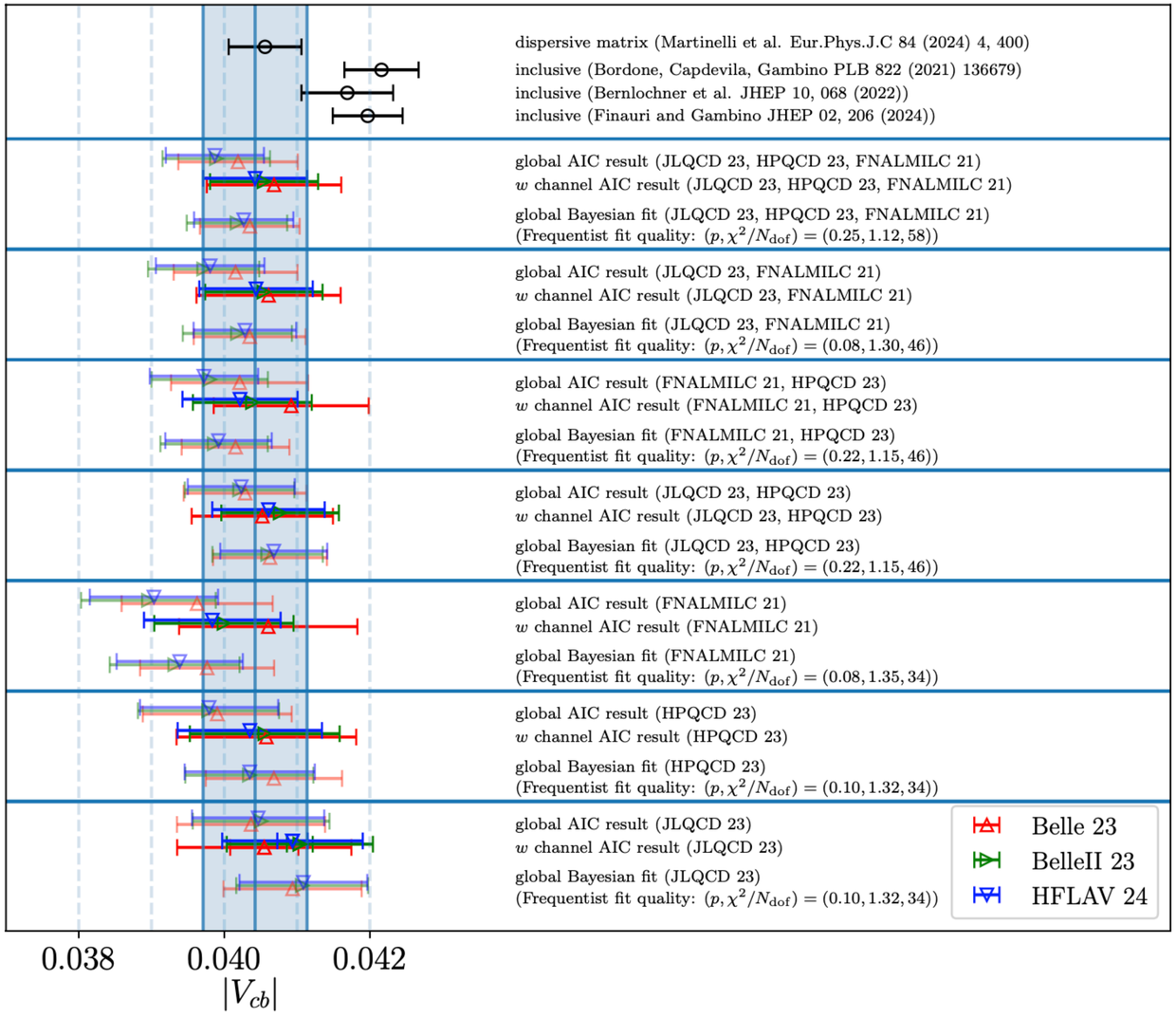

- comparison of different lattice and experimental input
- by and large good agreement (especially if angular bins discarded from AIC)

strategy A) BGL fit to lattice data, then combination with experiment

strategy B) BGL fit to both lattice and experiment

- **We find no noteworthy tensions between the results from both strategies**
- **This analysis confirms a slight tension with insclusive analyses**

Summary

Framework for truncation- and model-independent form-factor fitting
combining Frequentist and Bayesian statistics

Bayesian inference ansatz:

- Shown for $P \to P$ and $P \to V$ transitions
- Framework imposes unitarity constraint with meaningful statistical interpretation
- Unitarity constraint acts as regulator for higher-order coefficients
- Results converge to stable and truncation-independent values

- New quality of $B \to D^* \ell \bar{\nu}_\ell$ data from theory and experiment
- SM tests passed at current level of precision
- but our analysis shows tensions amongst lattice as well as experimental data sets
- $|V_{cb}|$ tension between inclusive and exclusive confirmed

Also have a look:

- Dispersive-matrix method, Di Carlo et al. PRD 2021, arXiv:2105.02497
- Self-consistency checks of z expansinon, Simons, Gustafson, Meurice arXiv:2304.13045

Thank you

Map q^2 to unit disk

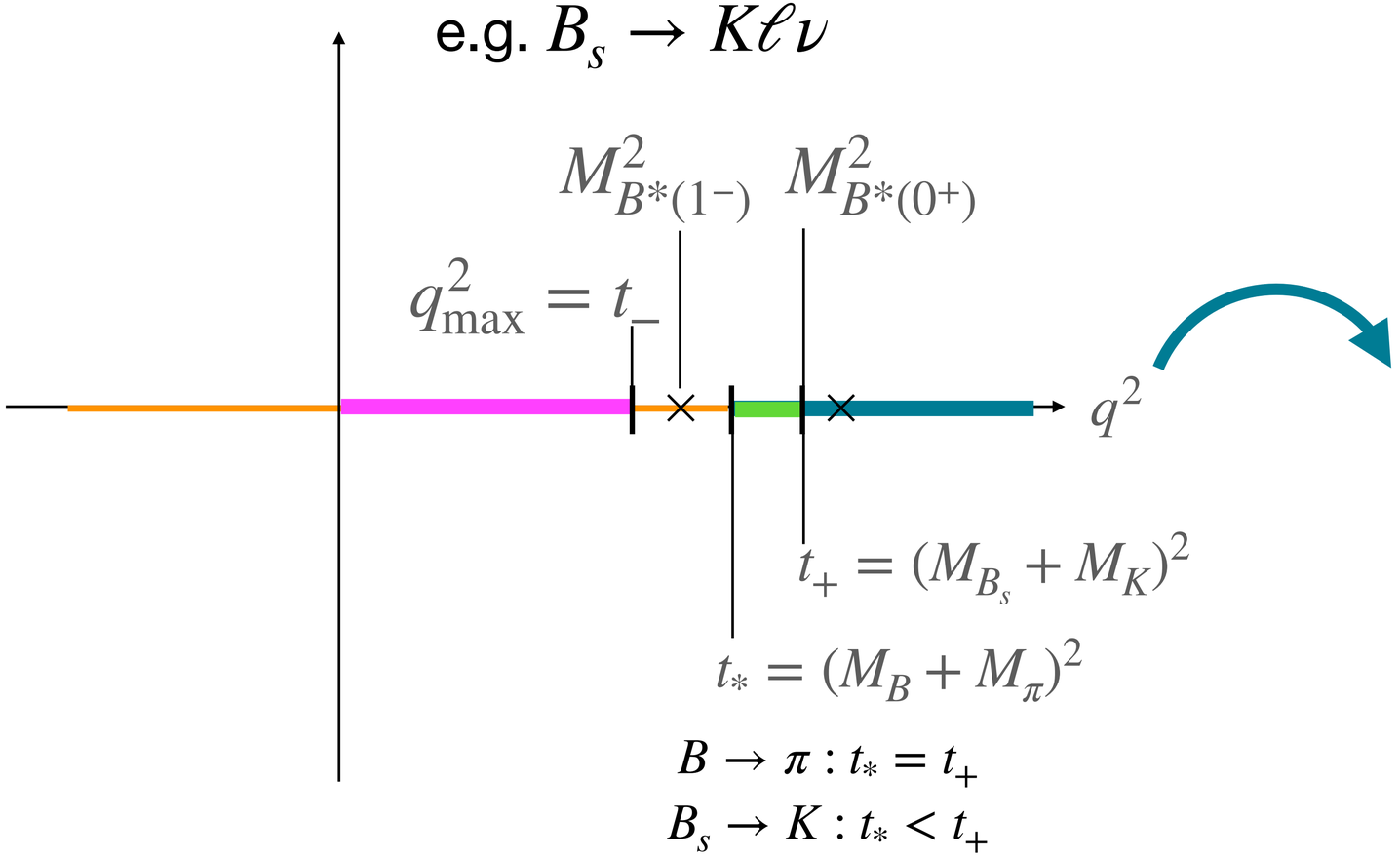

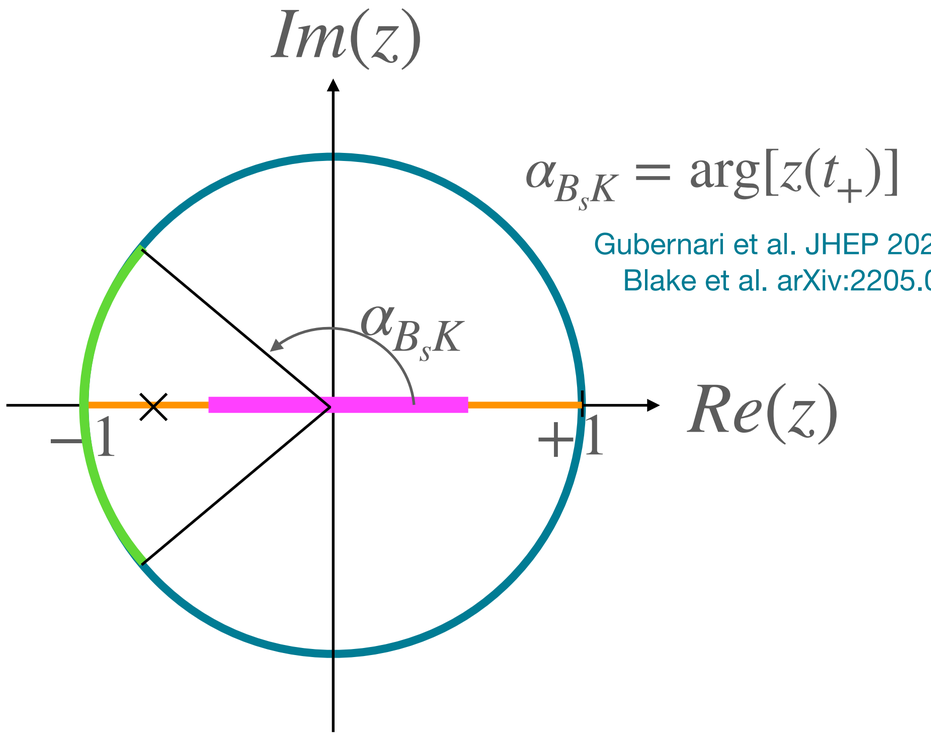

Gubernari et al. JHEP 2021,2022,
Blake et al. arXiv:2205.06041

Okubo, PRD 3, 2807 (1971), PRD 4, 725 (1971).
Okubo, Shih, PRD 4, 2020 (1971).
Boyd, Grinstein, Lebed, PLB 353, 306 (1995).
NPB461, 493 (1996). PRD 56, 6895 (1997).

BGL expansion

$$f_X(q_i^2) = \frac{1}{B_X(q_i^2)\phi_X(q_i^2, t_0)} \sum_{n=0}^{K_X-1} a_{X,n} z(q_i^2)^n \qquad X = +, 0$$

Boyd, Grinstein, Lebed, PRL 74 (1995)

unitarity constraint

$$\frac{1}{\pi\chi_J^T(q^2)} \int_{t_+}^{\infty} dt \frac{W(t)\,|f(t)|^2}{(t-q^2)^3} \leq 1 \quad \longrightarrow \quad \frac{1}{2\pi i} \oint_C \frac{dz}{z} \theta_{B_s K}\, |B_X(q^2)\phi_X(q^2, t_0) f_X(q^2)|^2 \leq 1$$

$$a_{X,i} \langle z^i \,|\, z^j \rangle a_{X,j} \leq 1$$

$$\langle z^i | z^j \rangle_\alpha = \frac{1}{2\pi} \int_{-\alpha}^{\alpha} d\phi (z^i)^* z^j |_{z=e^{i\phi}} = \begin{cases} \dfrac{\sin(\alpha(i-j))}{\pi(i-j)} & i \neq j \\ \dfrac{\alpha}{\pi} & i = j \end{cases}$$

Flynn, AJ, Tsang, arXiv:2303.11285

Bayesian Form factor Fit

Flynn, AJ, Tsang, arXiv:2303.11285

In practice high-dimensional → low probability of drawing random number compatible with constraint

$$\pi_{\mathbf{a}}(\mathbf{a}\,|\,\mathbf{f}_p, C_{\mathbf{f}_p})\pi_{\mathbf{a}}(\mathbf{a}\,|\,\mathbf{a}_p, M) \propto \theta(\mathbf{a})\exp\left(-\frac{1}{2}(\mathbf{f}_p - Z\mathbf{a})^T C_{\mathbf{f}_p}^{-1}(\mathbf{f}_p - Z\mathbf{a}) - \frac{1}{2}\mathbf{a}^T M/\sigma^2\,\mathbf{a}\right)$$

- Add ‘technical’ prior
- Choose M such that $\mathbf{a}^T M\mathbf{a} \leq 1$ in presence of kinematical constraint
- Correct towards ‘no-prior’ with accept-reject step with probability

$$p \leq \frac{\exp(-1/\sigma^2)}{\exp(-\mathbf{a}^T M\mathbf{a}/2\sigma^2)}$$

FINAL RESULT INDEPENDENT OF *TECHNICAL* PRIOR

FNAL/MILC 21 + HFLAV 23

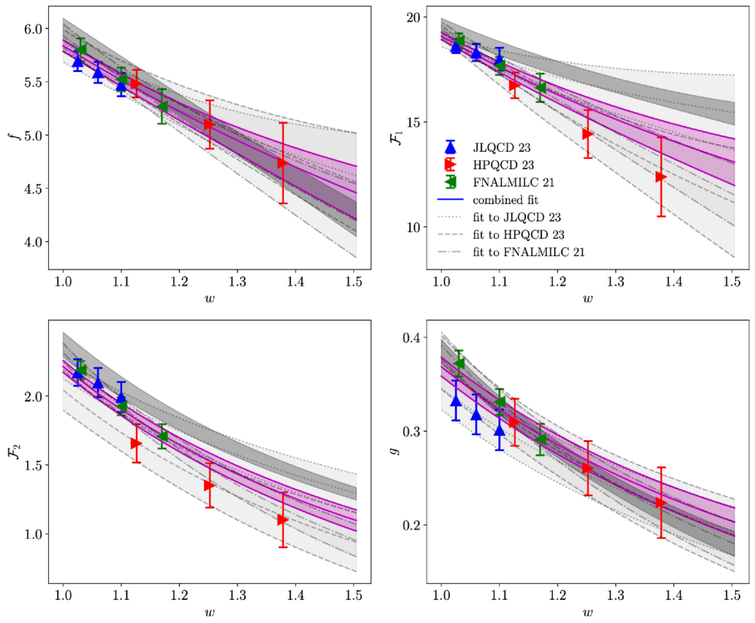

HPQCD 23 + HFLAV 23

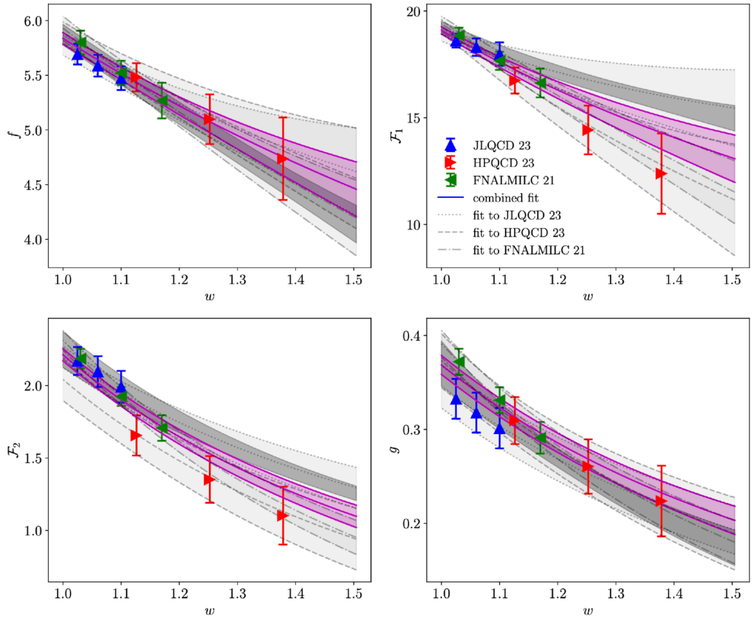

JLQCD 23 + HFLAV 23

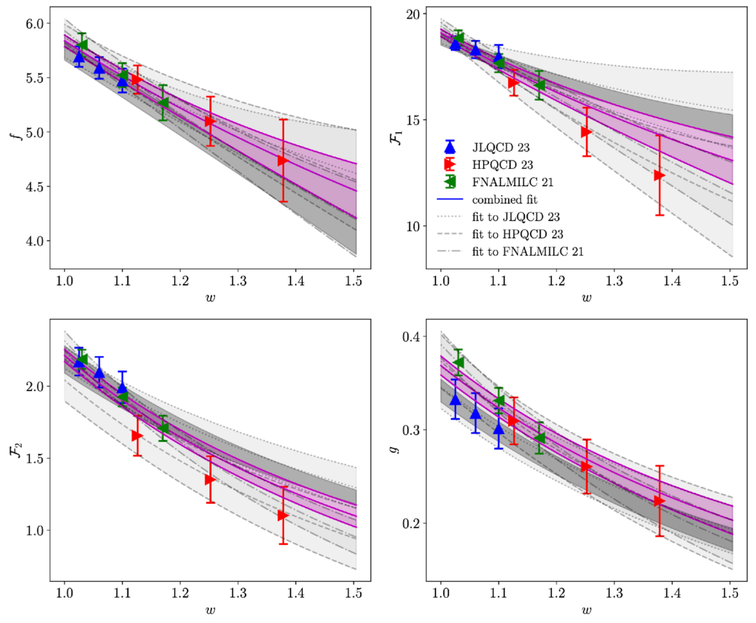

Example 1: $B_s \to K\ell\nu$ — fit to HPQCD 14

Distribution and correlation of BGL coefficients

truncation, e.g. $(K_+, K_0) = (5,5)$

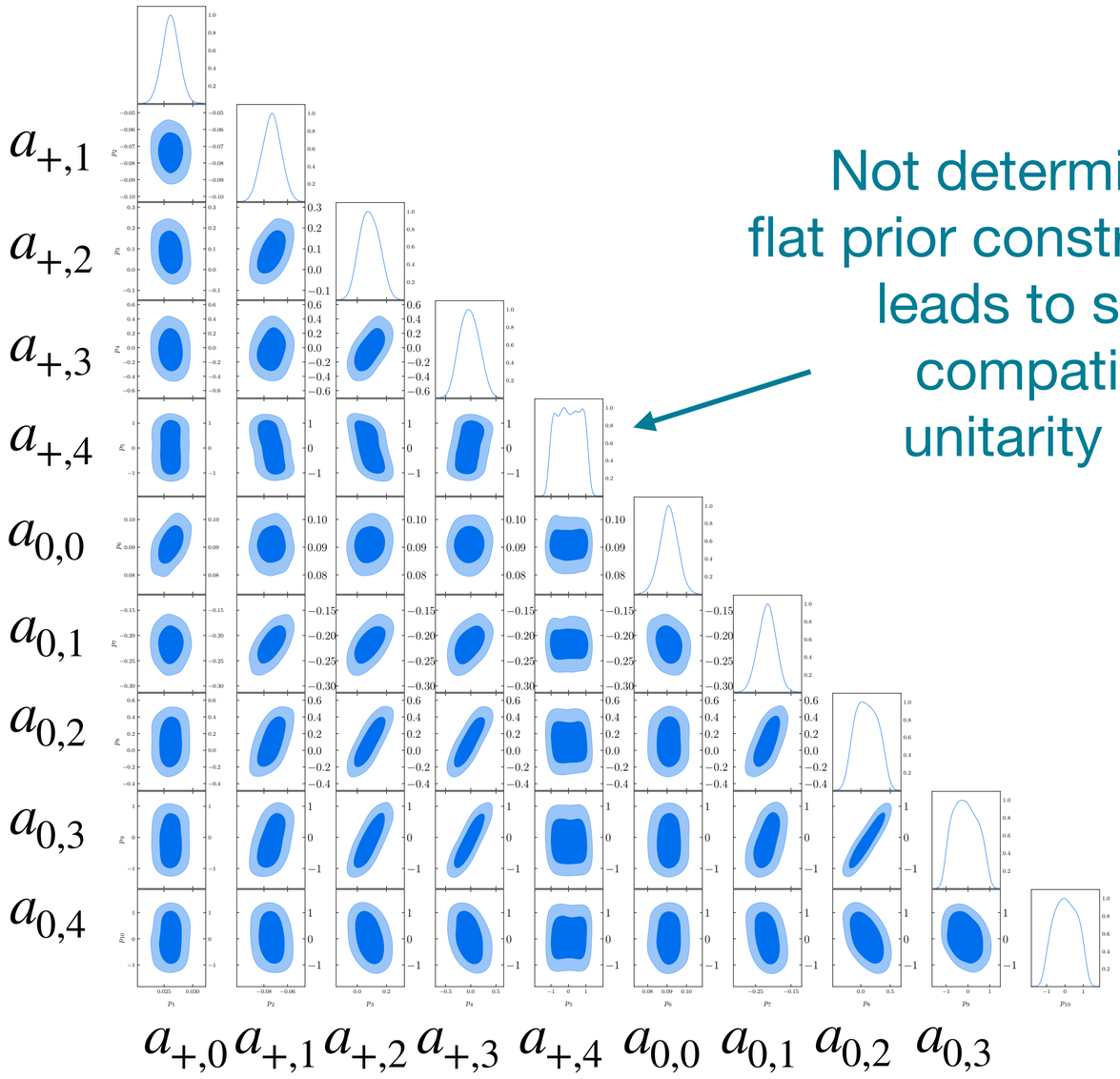

Not determined by data, flat prior constrains coefficient, leads to stability and compatibility with unitarity constraint